Comparison of the synoptic environment and the mechanisms of two cases of surface cyclogenesis in Greek area associated to strong low-level cold surges

ECMWF
UEF2016
Reading | 6-9 June 2016

John Kouroutzoglou[1,2] (ioankour@phys.uoa.gr), **Haralambos Karvelis[1]**, **Helena A. Flocas[2]**, **Maria Hatzaki[3]**, **Kleoniki Tsioutra[1]**, **Antonios Lalos[1]**, **Kevin Keay[4]**, and **Ian Simmonds[5]**

Overview

Cold surges propagating from North and Central Europe through the Balkans are frequently associated to the passage of fast moving cold fronts from the north (Prezerakos and Angouridakis, 1984). These are frequently linked with diabatic processes in the eastern Mediterranean, resulting in cyclogenesis (Flocas et al. 2010, Kouroutzoglou et al. 2011). The objective of this study is to examine the thermodynamic mechanisms at low and upper levels that are responsible for two cases of surface cyclogenesis at the Greek area, associated to strong low-level cold surges. Both cases were associated with strong weather phenomena, including strong snowfalls, gale force winds, and locally strong thunderstorms with different spatial distribution. The first synoptic case occurred over the southern Ionian Sea (from 29/12/2014 to 01/01/2015), while the second case over the southern Aegean Sea (from 11 to 13/01/2015).

Datasets

The datasets used in this study include:

- 6hr analyses from ERA-Interim (Dee et al. 2011), on 0.5° x 0.5° grid
- EUMESAT products, including the airmass composite RGB and severe storm RGB satellite images suitable for the detection of convective activity.
- thermal front parameter (hereafter TFP) and equivalent thickness overlaid upon the satellite images to depict the location of surface fronts

The above numerical weather products are available from Eumetsat and are based on the operational ECMWF forecast fields.

Synoptic environment

In the first case, upper tropospheric downstream development (Prezerakos et al. 1999) occurred on the eastern flanks of a blocking anticyclone in the Atlantic area, resulting in an organized large-scale trough over North Europe. At the same time, anticyclonic disruption of the respective large scale trough was observed in Central and North Europe, favouring upper-level cyclogenesis in the central Mediterranean. The cyclone followed a southern propagation (Fig. 1b) and became a cut-off over the Gulf of Syrte under the influence of the strong polar front jet, triggering surface cyclogenesis in the southern Ionian Sea (Fig.1a). In the second case, a large-scale upper-level anticyclone was established over the western Mediterranean, inducing the formation of a short-wave trough over Central Europe, favourable for rapid deepening during the next hours (Fig. 1d), over the Aegean Sea (Blumen 1979). The southward extension of the cold anticyclone from the Balkans was combined with the surface depression over the Aegean (Fig. 1c), while no cyclogenetic activity was observed in the Ionian Sea.

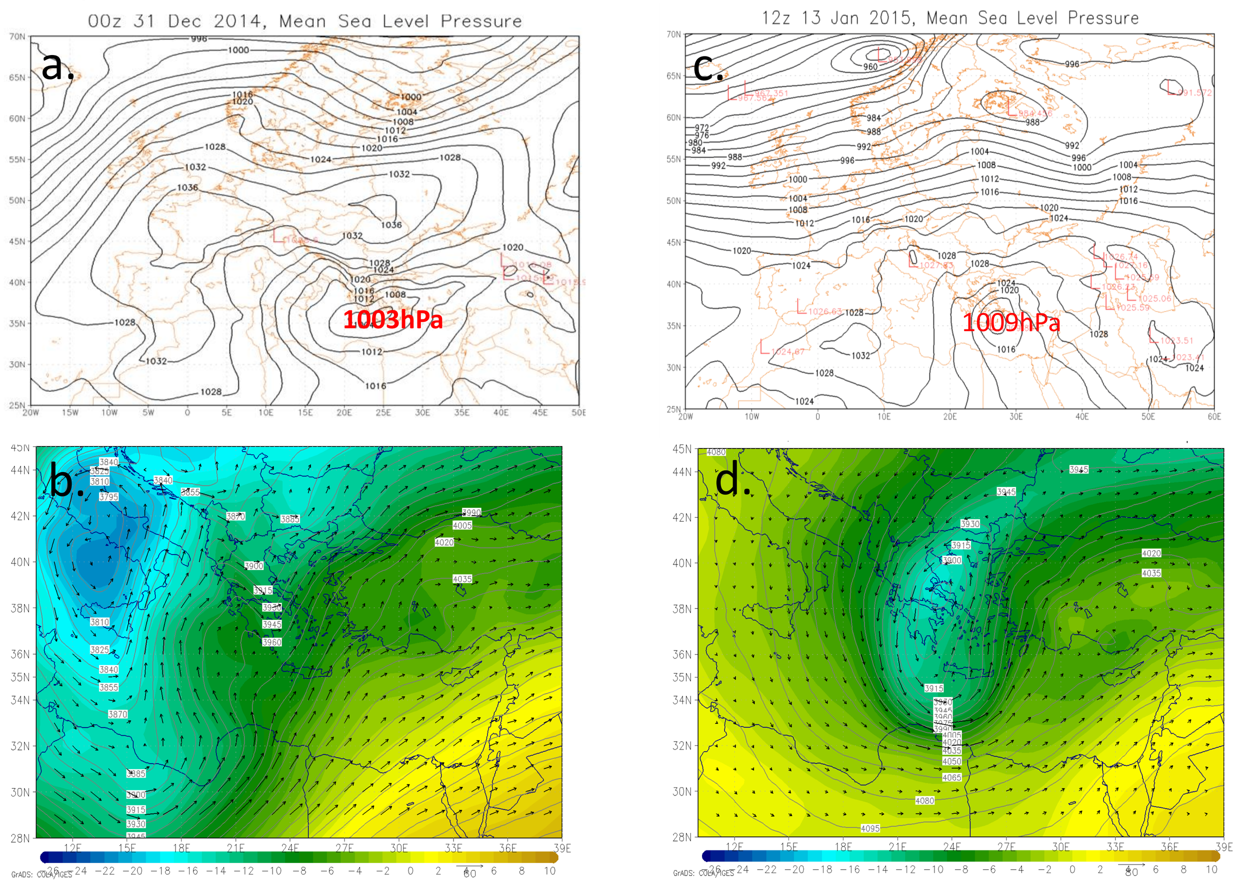

FIG.1. a, c) MSLP distribution at 31/00UTC and 13/12UTC, and b, d) Thermal wind and thickness 500-850hPa - 700hPa temperature at 31/12UTC and 13/00UTC. Contour intervals are 4hPa, 15 gpm, 5 ms^{-1} and 1°C, respectively. The unit vector is 60 ms^{-1}.

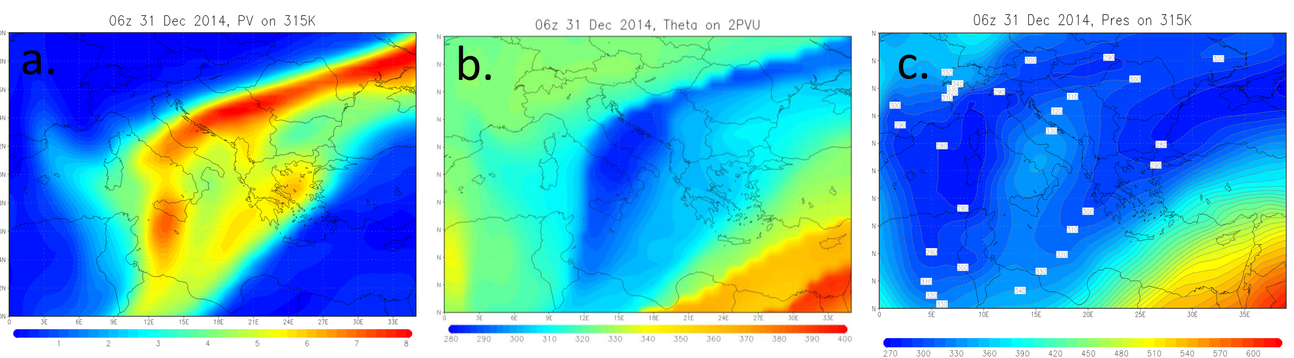

FIG.2. a) 315K PV, b) 2PVU theta and c) 315K pressure at 31/06UTC. Contour intervals are 0.1PVU, 2K, and 10hPa, respectively.

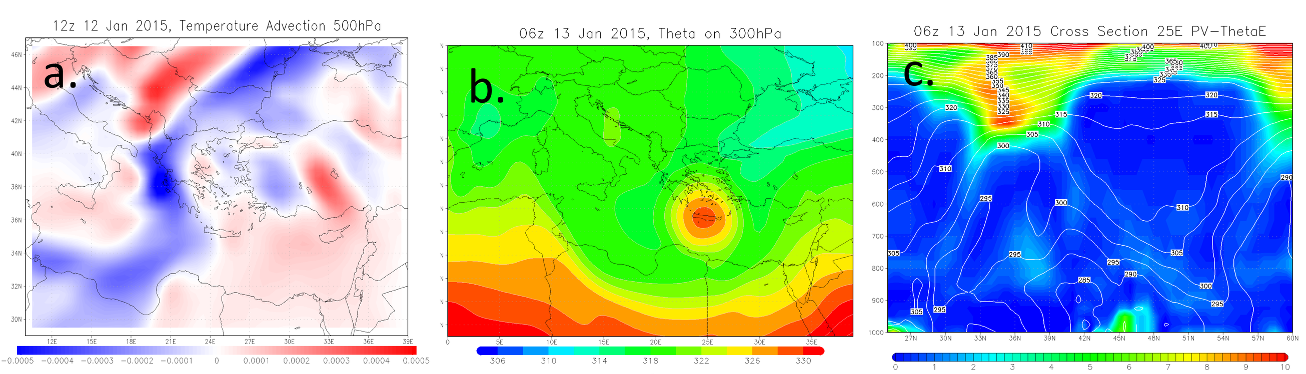

FIG.3. a) 500hPa temperature advection at 12/12UTC, b) 300hPa theta and c) PV-thetae cross-section at 25°E for 13/06UTC. Contour intervals are 10^{-5} °C/m, 2K , 0.2PVU and 5K , respectively.

Results

In both cases, intrusion of high-PV air of stratospheric origin at the dynamic tropopause level along with low-level warm air is depicted (Fig. 2 and 3). In the first case, the existence of an organized surface depression with enhanced frontal activities over the southern Ionian Sea and Aegean Seas (Fig. 7a) combined with the cold surface anticyclone over Greece, further increased low-level baroclinicity over eastern Greece. In the second case, upper tropospheric horizontal geostrophic vorticity and the thermal advection (Fig. 3a) also favoured surface cyclogenesis in the Aegean, which was further strengthened during its southward movement towards the southern Aegean, while the low-level baroclinicity in the Aegean was also strengthened due to the respective low-level cold surge from the Balkans towards the Greek area (Fig. 3b).

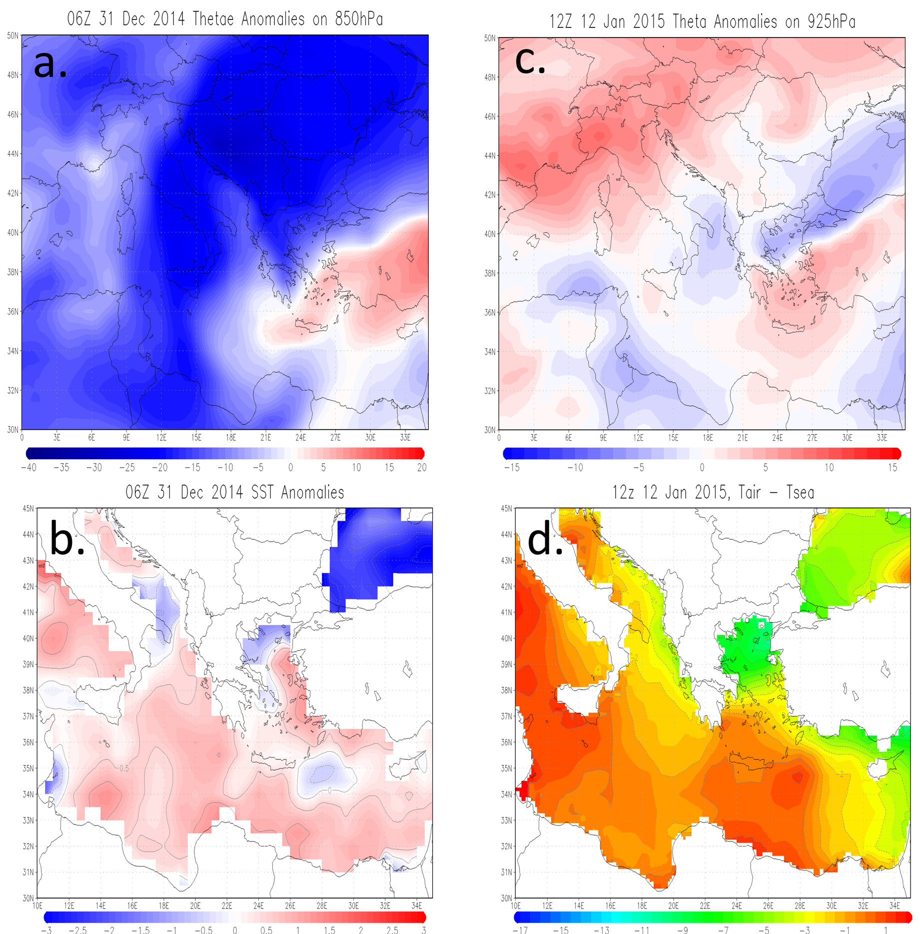

FIG.4. a, b) 850hPa theta and SST anomalies at 31/06UTC, c, d) 925 hPa theta anomalies and air-sea temperature differences at 12/12UTC. Contour intervals are 1 K for a and c, 0.5°C and 1°C for b and d, respectively.

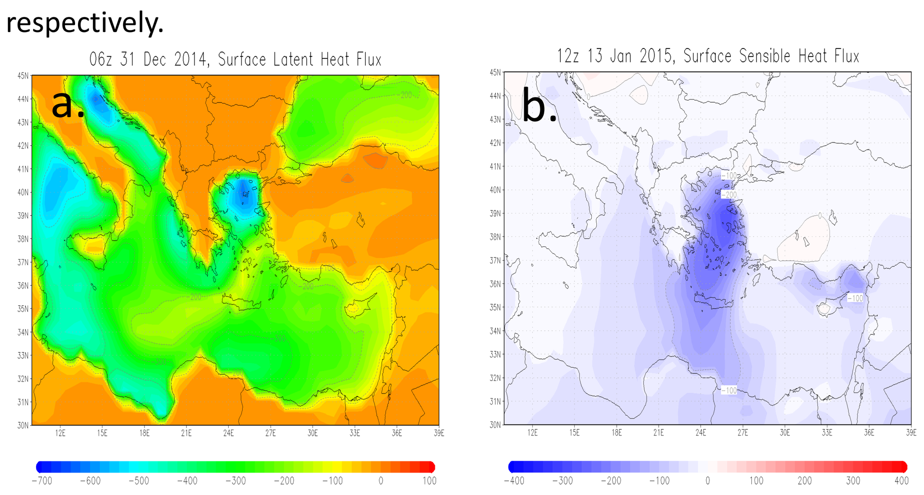

FIG.5. Surface a) latent heat flux at 31/06UTC and b) sensible heat flux at 13/12UTC. Contour intervals are 20W/m^2, respectively.

In the first case, moist, warm and potentially unstable air advected over the eastern continental parts (Fig. 4a), favouring the upglide strengthening of the warm air over the pre-existed cold, due to the propagation of the cold anticyclone from the Balkans towards Greece. Positive SST anomalies (Fig. 4b) formed over the Ionian Sea and the southeastern Aegean Sea between 30 and 31/12, while negative air-sea temperature differences covered the Greek area, peaking over the northern Aegean Sea, where strong cold-air advection occurs over the warmer maritime surface. Sensible and latent heat fluxes (Fig. 5) over the Ionian and Aegean Seas verified the above thermodynamic conditions.

Thus, low-level diabatic processes further interacted with the low-level convergence and baroclinicity, causing intense weather phenomena on eastern continental Greece (Fig. 6a).

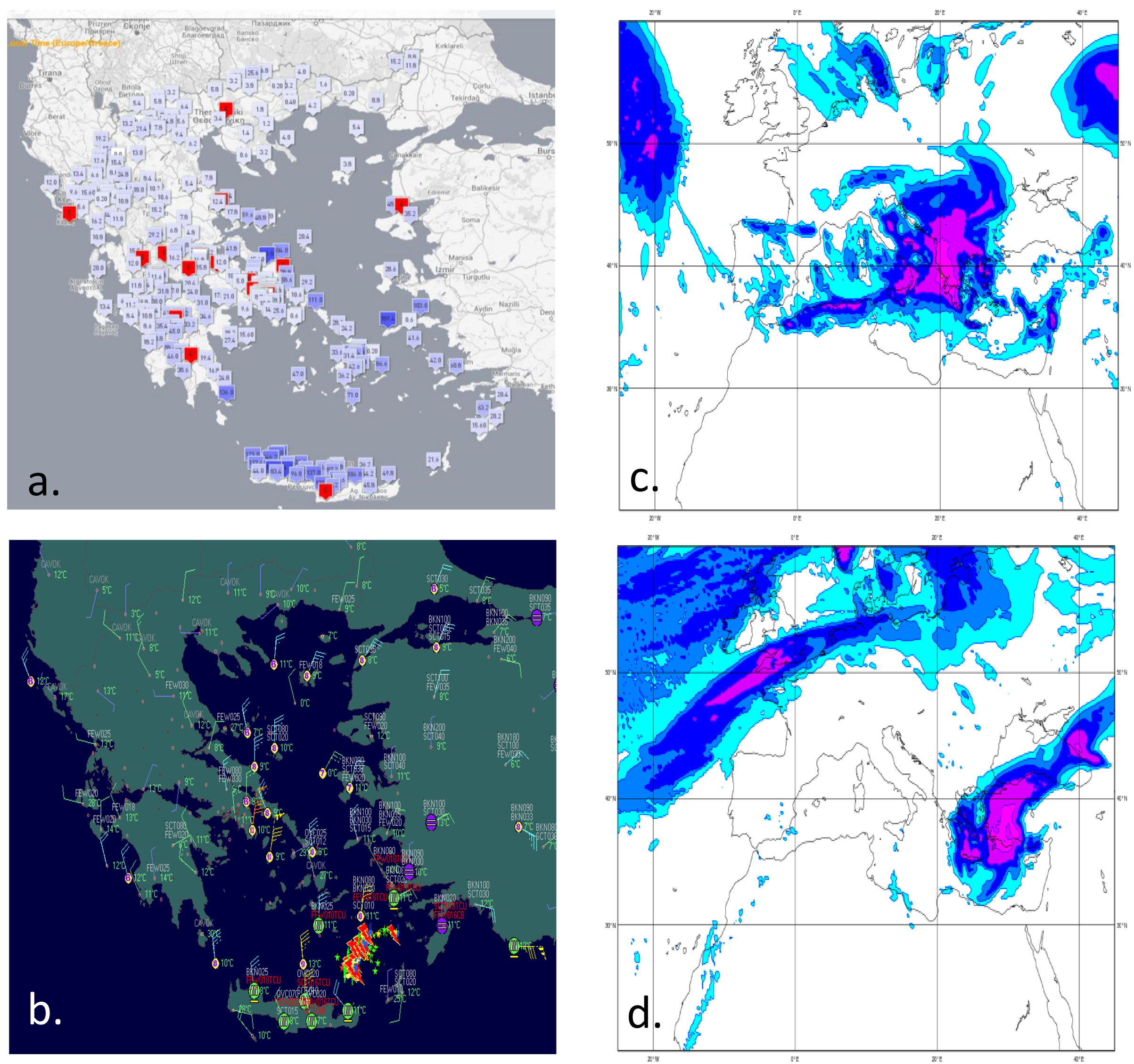

FIG.6. a) Total precipitation height in the Greek area between 29/12/2014 and 01/01/2015 in mm, b) Real time weather at 13/12UTC, c, d) 12hr accumulated total precipitation from the operational ECMWF model at 29/00UTC and 13/00UTC, respectively, in mm. In b green stars and red symbols denote thunderstorm activity.

In the second case, the surface cyclone propagated towards the southern Aegean and the winds shifted to N-NE. Nevertheless, the strengthening of low-level convergence and baroclinicity on the eastern continental parts, as observed in the previous case, was not the case for the distribution of the weather phenomena in this synoptic type, due to the absence of cyclonic activity to the west of Greece. Indeed, data from satellite images and the real-time weather demonstrate that the strongest phenomena were located over the Aegean Sea (Fig. 6b), followed by local snowfalls. Diabatic processes also favoured the cyclone's deepening during its southward movement towards the southern Aegean Sea, where it exhibited its minimum pressure (Fig. 4d, 5b). The low-level baroclinicity increased mainly over the southern Aegean (Fig. 4c), where strong thunderstorms associated to strong convection and local floods were observed in Crete (Fig. 6b, 7b), contrary to the first case where cyclogenesis in the southern Ionian Sea favoured the enhancement of convergence and low-level baroclinicity on the eastern continental parts, through the low-level wind shift into S-SE directions. Nevertheless, low-level diabatic heating sources at about the 850-750 hPa layer (Fig. 3c), were also found in this case, in the area of the Aegean Sea, where baroclinicity was enhanced (Lolis et al. 2004).

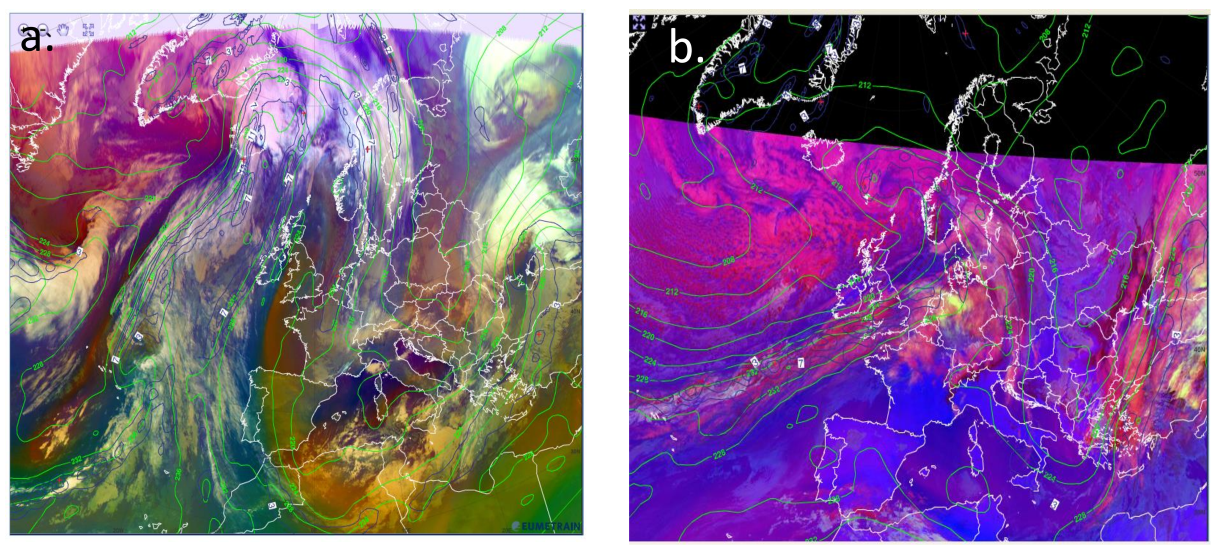

FIG.7. a) Air Mass Composite RGB satellite image along with equivalent thickness (green lines) and TFP (blues lines) for 29/18UTC and b) Severe storm RGB satellite image along with equivalent thickness (green lines) and TFP (blues lines) for 30/06UTC. Both images with the ECMWF NWP are provided by Eumetsat.

Conclusions

Although both cases exhibited similarities in the evolution of the respective synoptic environment and the mechanisms in the upper and lower troposphere, significant differences were observed. The existence of an organized frontal depression in the southern Ionian Sea in the first case seems to be the crucial factor that determined the strength of low-level pressure gradient, the magnitude of the cold surge over Greece and the intensity of the weather phenomena on eastern continental Greece, through the strengthening of low-level convergence and baroclinicity. For both cases, the precipitation maxima and their spatial distribution (Fig. 6 c,d) verified that the operational ECMWF model simulated effectively the cyclones evolution and the respective thermodynamic mechanisms.

These two synoptic cases that consist, as well, distinct categories of synoptic types that influence the Greek area during the cold period of the year, stress the ability of a global model, like the operational ECMWF model, to effectively capture the smaller scale cyclogenesis in the Mediterranean Sea and its impact on areas with complex topographical characteristics, which affect the observed precipitation.

References: Blumen, 1979: J Atmos Sci 36: 1925–1933 // Dee et al., 2011: Q J R Meteorol Soc 137, 553–597 // Flocas et al, 2010: J Clim 23:5243–5257 // Kouroutzoglou et al, 2011: Int J Climatol 31:1785–1802 // Lolis et al, 2004: Int J Climatol 24:1803-1816 // Prezerakos and Angouridakis, 1984: Int J Climatol 4:269–285 // Prezerakos et al, 1999: Meteorol Appl 6:1–10

[1] Hellenic National Meteorological Service
Helliniko, Athens, 16777, Greece

[2,3] National and Kapodistrian University of Athens
Dept. of Environmental Physics – Meteorology, Faculty of Physics, 157 84 Athens, Greece
Dept. of Geology and Geoenvironment, Faculty of Geology and Climatology

[4] Bureau of Meteorology
Melbourne, Victoria, Australia

[5] The University of Melbourne
Melbourne, Victoria, Australia